

Solid Phase Equilibrium Relations in the CaO-SiO₂-Nb₂O₅-La₂O₃ System at 1273 K



Jiyu Qiu and Chengjun Liu

Silicate slag system with additions Nb and RE formed in the utilization of REE-Nb-Fe ore deposit resources in China has industrial uses as a metallurgical slag system. The lack of a phase diagram, theoretical, and thermodynamic information for the multi-component system restrict the comprehensive utilization process. In the current work, solid phase equilibrium relations in the CaO-SiO₂-Nb₂O₅-La₂O₃ quaternary system at 1273 K (1000 °C) were investigated experimentally by the high-temperature equilibrium experiment followed by X-ray diffraction, scanning electron microscope, and energy dispersive spectrometer. Six spatial independent tetrahedron fields in the CaO-SiO₂-Nb₂O₅-La₂O₃ system phase diagram were determined by the Gibbs Phase Rule. The current work combines the mass fraction of equilibrium phase and corresponding geometric relation. A determinant method was deduced to calculate the mass fraction of equilibrium phase in quaternary system according to the Mass Conservation Law, the Gibbs Phase Rule, the Lever's Rule, and the Cramer Law.

<https://doi.org/10.1007/s11663-017-1144-0>

© The Minerals, Metals & Materials Society and ASM International 2017

I. INTRODUCTION

CHINA'S Inner Mongolia contains a large rare earth element-Nb-Fe complex ore deposit: Bayan Obo REE-Nb-Fe. Extracting valuable elements from the REE-Nb-Fe ore deposit imposes difficulties due to the multiple-element symbiotic specificity. Until now, niobium and rare earth resources were wasted as tailings in the ore dressing process, which led to a huge waste of resources.^[1] Processes and techniques to smelt metal niobium and enrich rare earth resources from the tailings have been proposed, but the processes have flaws in the low metal yield and high cost. The uncertainties of thermodynamic property especially the phase diagram data for the tailings with niobium and rare earth severely restrict the development of above mentioned processes.^[2] In correlative slag phase diagrams, CaO-SiO₂-Nb₂O₅ ternary system had been investigated by Jongejan and Wilkins.^[3] Previous work did not study the phase diagram for the slag system with Nb and REE. Phase relations for the slag system with REE and Nb remain unclear, making it necessary to update the fundamental thermodynamic information for

the development and application of processing the slag. The CaO-SiO₂-Nb₂O₅-La₂O₃ system contains the most directly related slag system during the pyrometallurgy extraction process of niobium and rare earth resources in REE-Nb-Fe ore deposit.

The most common scientific method for the investigation of silicate system phase diagrams uses the high-temperature equilibrium experiment.^[4-7] Relations between equilibrium phases and the corresponding proportion relation contain important thermodynamic information in phase diagram.^[8] Little research exists for the proportion relation of equilibrium phases in a multi-component system. This also limits the study on multi-component system phase diagram.

In the current work, solid phase equilibrium relations and corresponding proportion relation in the CaO-SiO₂-Nb₂O₅-La₂O₃ system within the specified region were determined experimentally by the high-temperature equilibrium experiment followed by the X-ray diffraction (XRD), the scanning electron microscope (SEM), and the energy dispersive spectroscope (EDS) analysis. The current research provides significant results for the quaternary system and application of multi-component system phase diagram with benefits to the comprehensive utilization for niobium and rare earth resources.

II. EXPERIMENT

In this section, we describe the preparation and equilibrium experiments for determining solid phase

Jiyu Qiu and Chengjun Liu are with the Key Laboratory for Ecological Metallurgy of Multimetallic Ores (Ministry of Education), Wenhua Road, Heping District, Shenyang 110819, Liaoning Province, China and also with the School of Metallurgy, Northeastern University, Wenhua Road, Heping District, Shenyang 110819, Liaoning Province, China. Contact email: liucj@smm.neu.edu.cn

Manuscript submitted March 9, 2017.

Article published online December 5, 2017.

equilibrium relations in the CaO-SiO₂-Nb₂O₅-La₂O₃ quaternary system.

A. Sample Preparation

Reagent grade oxide powders (provided by the Sinopharm Chemical Reagent Co., Ltd.) of CaO (99.99 mass fraction pure), SiO₂ (99.99 mass fraction pure), Nb₂O₅ (99.99 mass fraction pure), and La₂O₃ (99.99 mass fraction pure) were used to prepare the slags, which were calcined at 1273 K (1000 °C) for 14,400 seconds to evaporate the moisture and impurities. 0.015 kg mixtures were carefully weighed, fully mixed, and pre-melted in air atmosphere using MoSi₂ furnace. The mixtures were placed inside platinum crucibles and placed inside the furnace at 1873 K (1600 °C) for 21,600 seconds to completely homogenize the slags. The size of platinum crucibles for pre-melt has an upper diameter 0.04 m, bottom diameter 0.03 m, and height 0.038 m. The pre-melt time was decided by pre-experiment by determining that 21,600 seconds was enough to achieve the homogenization of slag. After homogenization of the slag, the samples were quenched into ice-water, dried, crushed, and ground to 200 meshes for further use. Temperature was monitored by a B-type thermocouple placed next to the samples with an overall temperature accuracy estimated to 2 K.

The pre-melt slag was analyzed by XRD and SEM to ensure the effect of pre-melt experiments, the EDS result, as listed in Table I, was used as the initial composition of pre-melt slag. Quenching by ice-water ensured that the quenched slags showed glassy phase, as shown in Figures 1 and 2. The pre-melt results showed that 1873 K (1600 °C) achieved the homogenization of slag samples. The compositions of pre-melt slag measured by EDS are projected on the CaO-SiO₂-Nb₂O₅-10 wt pct La₂O₃ pseudo-ternary phase diagram, as shown in Figure 3.

B. Equilibrium Experiments

The MoSi₂ furnace used for the pre-melt was also used for the equilibrium experiment. The pre-melt slag (0.0015 kg for each slag) was placed in the platinum crucible and placed into the hot zone of the MoSi₂

furnace. The curve of controlled temperature was shown in Figure 4. It was found that the complete crystallization temperature of each slag was above 1273 K in pre-experiment, in order to ensure that each slag could crystallize completely, the equilibrium temperature in the equilibrium experiment was determined to be 1273 K (1000 °C). The equilibration time lasted 86,400 seconds based on experiences reported by previous authors,^[9-12] repeat experiments with 172,800 seconds were performed for some samples to check whether the equilibrium was achieved. There was no significant difference between the equilibrium phases with longer equilibration time. After the equilibrium, the sample was rapidly taken out from the furnace and quenched to 273 K (0 °C) by ice-water, the quenching process was completed in 2 seconds to ensure that all samples maintained the high-temperature equilibrium phase composition and construction. Quenched samples were dried and embedded in epoxy resin and polished for analysis. SEM, XRD, and EDS were used to identify the phase equilibrium relations and analyze the composition of each phase in the samples.

III. RESULTS AND DISCUSSION

We discuss details related to the equilibrium phase relations at 1273 K, determine independent tetrahedron, and perform quantitative analysis on each equilibrium phase.

A. Equilibrium Phase Relations at 1273 K

The microstructure and composition of the equilibrium phases at 1273 K (1000 °C) are shown in Table II and Figure 5, respectively. The composition of the equilibrium phase has been composed of the average values calculated from six different analysis points in the sample. Figure 5(a) shows the four phases that were detected by SEM for sample #1, based on the XRD result of sample #1 we can confirm that the black phase consists of SiO₂, the deep gray phase consists of CaO·Nb₂O₅, the white phase consists of La₂O₃·6Nb₂O₅, and the light gray phase consists of Nb₂O₅. Based on the EDS results, elemental calcium was found in the

Table I. The Comparison of Designed and EDS Measured Compositions of Pre-melt Slags (Mass Pct)

Slag Nos.	CaO (Pct)	SiO ₂ (Pct)	Nb ₂ O ₅ (Pct)	La ₂ O ₃ (Pct)
#1				
Designed	4.82	3.32	81.86	10.00
EDS	4.23	3.42	81.06	11.29
#2				
Designed	29.11	38.89	22.00	10.00
EDS	26.89	38.53	22.42	12.16
#3				
Designed	20.55	12.03	57.42	10.00
EDS	20.08	12.87	56.97	10.08
#4				
Designed	31.54	20.46	38.00	10.00
EDS	30.74	20.94	38.55	9.77

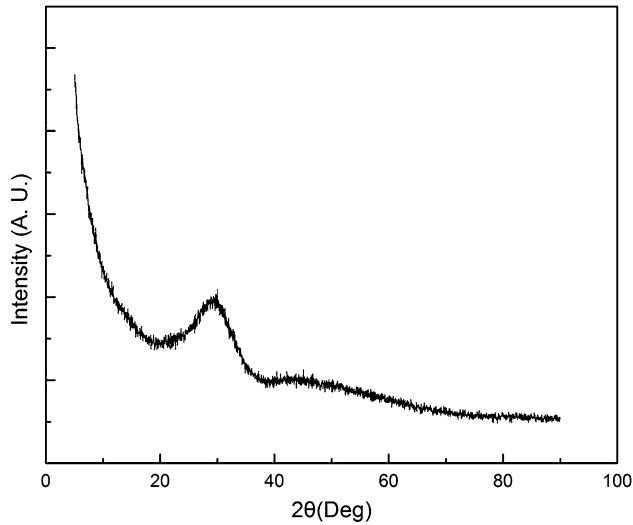


Fig. 1—XRD result of typical pre-melt slag.

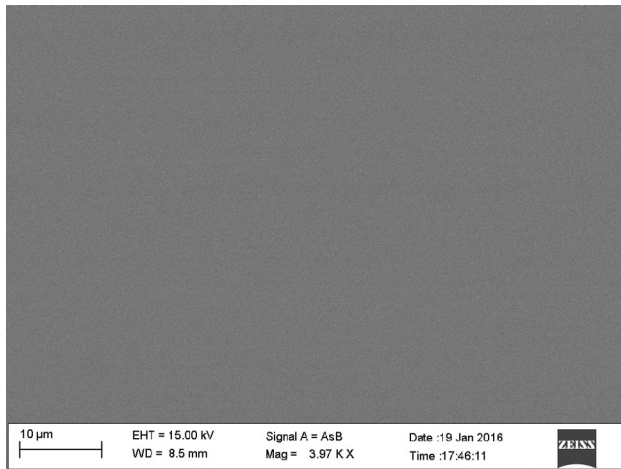


Fig. 2—Backscattered electron image of typical pre-melt slag.

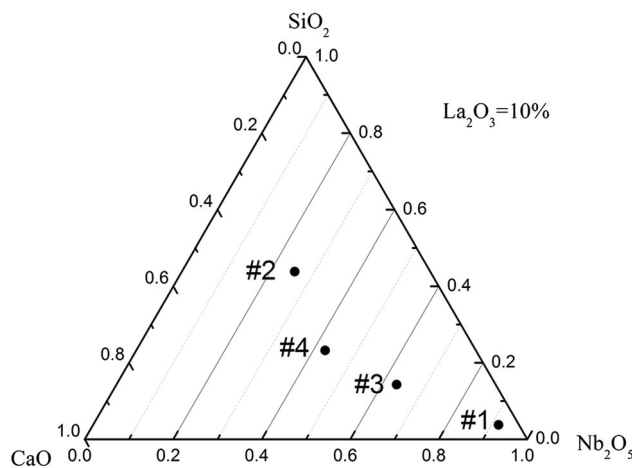


Fig. 3—The projection of pre-melt compositions on CaO-SiO₂-Nb₂O₅-10 wt pct La₂O₃ pseudo-ternary phase diagram.

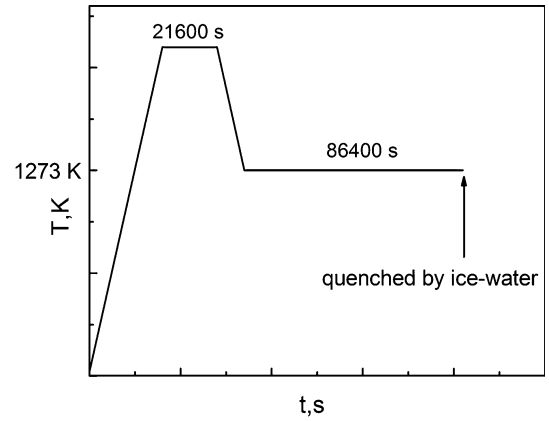


Fig. 4—Curve of controlled temperature in high-temperature equilibrium experiment.

composition of La₂O₃·6Nb₂O₅, and elemental lanthanum was found in the composition of CaO·Nb₂O₅ and 2CaO·Nb₂O₅. Frolov and Evdokimov^[13] found that elemental calcium can be dissolved in La₂O₃·6Nb₂O₅ and elemental lanthanum can be dissolved in CaO·Nb₂O₅ and 2CaO·Nb₂O₅ within a certain composition range. In Figure 5(b), four phases were detected by SEM for sample #2, we confirm that the light gray with strip shape consists of CaO·Nb₂O₅, the black phase consists of SiO₂, the white phase with block shape consists of La₂O₃·Nb₂O₅, and the deep gray phase consists of CaO·SiO₂. In Figure 5(c), four phases were detected by SEM for sample #3, based on the XRD result, we confirm that the black phase consists of CaO·SiO₂, the gray phase with strip shape consists of CaO·Nb₂O₅ and 2CaO·Nb₂O₅, the white phase consists of La₂O₃·Nb₂O₅. The SEM microphotographs show no difference in morphology and contrast between CaO·Nb₂O₅ and 2CaO·Nb₂O₅. In Figure 5(d), four phases were detected by SEM for sample #4, based on the XRD result of #4, we confirm that the gray phase with strip shape consists of 2CaO·Nb₂O₅, the black phase consists of CaO·SiO₂, the white phase with block shape consists of La₂O₃·Nb₂O₅, and the deep gray phase consists of 10CaO·6SiO₂·Nb₂O₅. The CaO-SiO₂-Nb₂O₅ ternary compound, known as “Niocalite”, was first discovered by Nickel.^[14] Elemental lanthanum was detected in the 10CaO·6SiO₂·Nb₂O₅ using EDS in the current experiment.

B. Determination of Independent Tetrahedron

Under the constant pressure condition, the Gibbs Phase Rule for the system can be expressed as Formula (1).

$$F = C - P + 1. \quad [1]$$

The terms F , C , and P in Formula (1) are the number of degrees of freedom, components, and equilibrium phases,^[15] respectively. The completely crystallized temperature for the system approaches T_s under constant pressure conditions. When T is less than T_s and the solid phase decomposition did not appear in the system, the

Table II. Experimental Determined Phase Compositions of Equilibrium Phase at 1273 K (1000 °C) in CaO-SiO₂-Nb₂O₅-La₂O₃ System

Slag Nos.	Contrast in the SEM Microphotograph	Phases	Composition (Mass Pct)			
			CaO	SiO ₂	Nb ₂ O ₅	La ₂ O ₃
#1	black	SiO ₂	—	100	—	—
	deep gray	CaO·Nb ₂ O ₅	10.90	—	82.77	6.33
	white	La ₂ O ₃ ·6Nb ₂ O ₅	1.48	—	84.03	14.49
	light gray	Nb ₂ O ₅	—	—	100.00	—
#2	light gray	CaO·Nb ₂ O ₅	13.96	—	86.04	—
	deep gray	CaO·SiO ₂	41.79	58.21	—	—
	black	SiO ₂	—	100.00	—	—
	white	La ₂ O ₃ ·Nb ₂ O ₅	5.41	—	42.28	52.31
#3	black	CaO·SiO ₂	48.82	51.18	—	—
	gray	CaO·Nb ₂ O ₅	10.67	—	83.44	5.84
	gray	2CaO·Nb ₂ O ₅	21.09	—	70.91	8.01
	white	La ₂ O ₃ ·Nb ₂ O ₅	2.84	—	45.46	51.69
#4	gray	2CaO·Nb ₂ O ₅	19.50	—	72.64	7.86
	black	CaO·SiO ₂	46.01	53.99	—	—
	white	La ₂ O ₃ ·Nb ₂ O ₅	9.00	—	43.13	47.87
	deep gray	10CaO·6SiO ₂ ·Nb ₂ O ₅	40.33	30.11	25.96	3.60

degree of freedom could be represented as the uniform function of the temperature, implying that the number of components equal the number of equilibrium phases. Table III shows the relationship between “C”, “F”, and “P”. It can be seen that four equilibrium solid phases coexist in the CaO-SiO₂-Nb₂O₅-La₂O₃ system at $T < T_s$.

According to the equilibrium experiment results and the compatibility of phase diagram, six independent tetrahedron fields in the CaO-SiO₂-Nb₂O₅-La₂O₃ system were determined, as shown in Table IV and Figure 6. The Tetrahedrons ⑤ and ⑥ were determined by the Tetrahedrons ① and ② according to the existing phase information in related sub-systems^[16,17] and the compatibility of phase diagram.

C. Quantitative Analysis of Each Equilibrium Phase

After the determination of an independent tetrahedron field in the spatial phase diagram, for any component point in it at T lower than T_s , proportion relation of the equilibrium solid phases could be calculated by the relative position of the initial component point and the related equilibrium phase. However, due to the quaternary tetrahedral phase, diagram cannot be represented by a flat graphic. In the current work, we present a determinant calculation method to evaluate whether a given component point exists in a certain tetrahedral field in the quaternary system phase diagram. Using the determinant calculation, the proportion relation of the equilibrium phases can also be calculated. The relevant steps and principles of the determinant calculation method will be introduced using the example quaternary system.

As shown in Figure 7, A, B, C, and D represent the four hypothetical basic phases of the A-B-C-D quaternary system. M, N, P, and Q represent the equilibrium phases involved in the related tetrahedron field. The initial composition of sample E, involved in the discussion as an example, is that mass pct A = A_E ,

mass pct B = B_E , mass pct C = C_E , and mass pct D = D_E . Table V shows the theoretical composition of phases M, N, P, and Q. We can then construct the determinant V as represented in Formula (2).

$$V = \begin{vmatrix} 1 & 1 & 1 & 1 & 1 \\ A_M & A_N & A_P & A_Q & A_E \\ B_M & B_N & B_P & B_Q & B_E \\ C_M & C_N & C_P & C_Q & C_E \\ D_M & D_N & D_P & D_Q & D_E \end{vmatrix}. \quad [2]$$

Set $V_M = |A_{11}|$, $V_N = |A_{12}|$, $V_P = |A_{13}|$, $V_Q = |A_{14}|$, and $V_E = |A_{15}|$, that are the absolute value of the “algebraic cofactor” of each element in the first row of the determinant in Formula (2), as shown in Formula (3) for example.

$$|A_{11}| = \begin{vmatrix} A_N & A_P & A_Q & A_E \\ B_N & B_P & B_Q & B_E \\ C_N & C_P & C_Q & C_E \\ D_N & D_P & D_Q & D_E \end{vmatrix}. \quad [3]$$

When the equation $V_M + V_N + V_P + V_Q = V_E$ holds, sample E exists inside the tetrahedral field M-N-P-Q and its low temperature equilibrium phases are M, N, P, and Q. (Of course the equation holds in the discussion due to the initial setup.) Moreover, the equilibrium mass fraction of phases M, N, P, and Q is $\frac{V_M}{V_E} \times 100$ pct, $\frac{V_N}{V_E} \times 100$ pct, $\frac{V_P}{V_E} \times 100$ pct and $\frac{V_Q}{V_E} \times 100$ pct, respectively. The equilibrium mass fraction of the M phase equals the volume ratio of the tetrahedron N-P-Q-E and the tetrahedron M-N-P-Q. Intuitively, the mass fraction of each equilibrium phase could be determined by the volume ratio of the related tetrahedrons. The physical meaning of this equivalence process can be the theoretical *Spatial Lever Rule*.

We will now derive the Spatial Lever Rule, Figure 8, as a spatial tetrahedron representing a quaternary

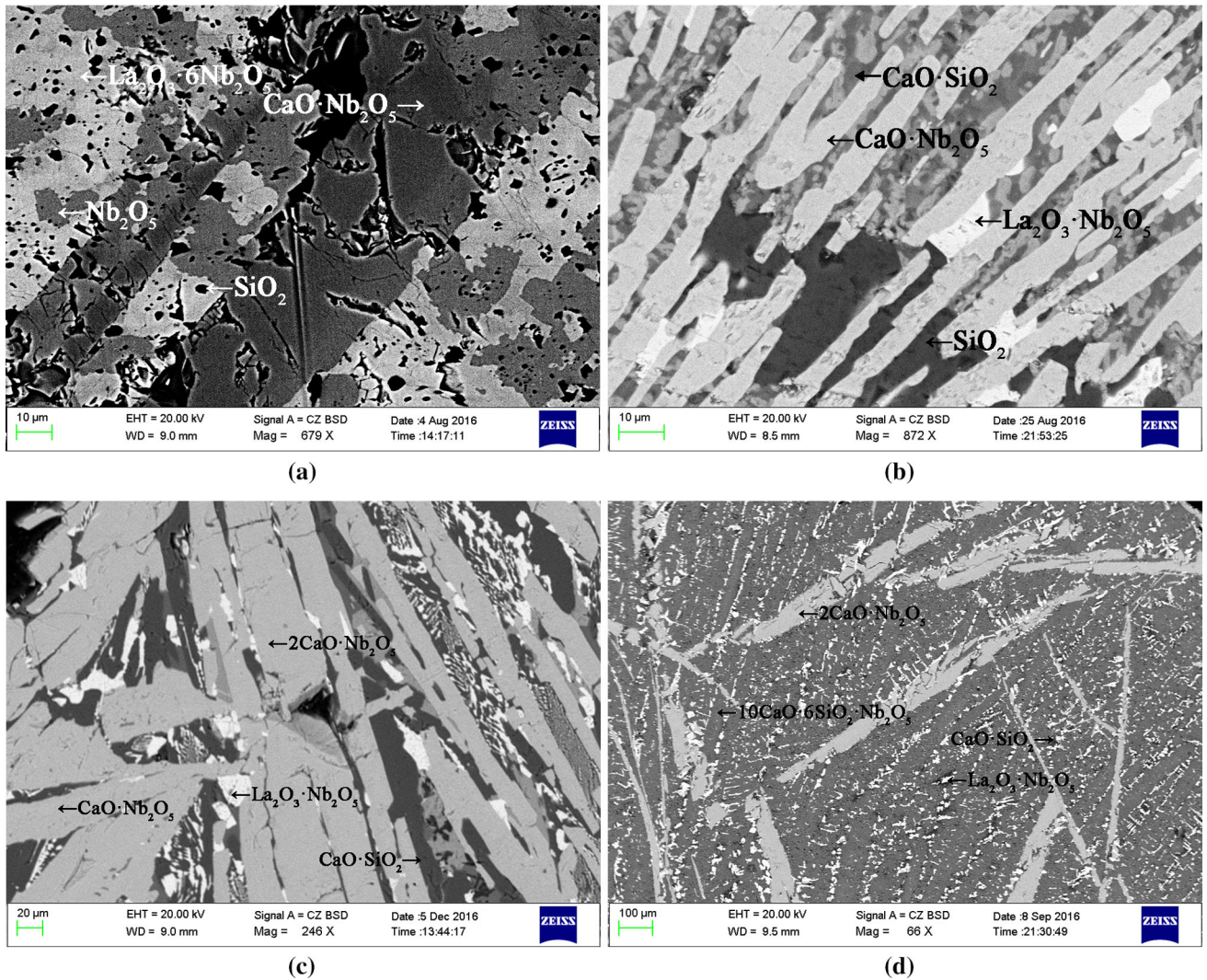


Fig. 5—SEM microphotographs of equilibrium phases at 1273 K (1000 °C).

Table III. Relationship Between *C* and *P* in Silicate System with Constant Pressure and $T < T_s$

<i>C</i>	Single-Component	Binary	Ternary	Quaternary	<i>n</i> -Component
Phase Rule	$F = 1 - P + 1$	$F = 2 - P + 1$	$F = 3 - P + 1$	$F = 4 - P + 1$	$F = n - P + 1$
<i>P</i>	1	2	3	4	<i>n</i>

Table IV. Independent Tetrahedron Fields in the CaO-SiO₂-Nb₂O₅-La₂O₃ System

Tetrahedron Nos.	The Solid Phases Involved in Tetrahedron
①	SiO ₂ -CaO-Nb ₂ O ₅ -Nb ₂ O ₅ -La ₂ O ₃ -6Nb ₂ O ₅
②	La ₂ O ₃ ·Nb ₂ O ₅ -CaO·SiO ₂ -SiO ₂ -CaO·Nb ₂ O ₅
③	La ₂ O ₃ ·Nb ₂ O ₅ -CaO·SiO ₂ -CaO·Nb ₂ O ₅ -2CaO·Nb ₂ O ₅
④	La ₂ O ₃ ·Nb ₂ O ₅ -CaO·SiO ₂ -10CaO·6SiO ₂ ·Nb ₂ O ₅ -2CaO·Nb ₂ O ₅
⑤	La ₂ O ₃ ·3Nb ₂ O ₅ -CaO·Nb ₂ O ₅ -SiO ₂ -La ₂ O ₃ ·Nb ₂ O ₅
⑥	La ₂ O ₃ ·3Nb ₂ O ₅ -CaO·Nb ₂ O ₅ -SiO ₂ -La ₂ O ₃ ·6Nb ₂ O ₅

system. A component point, as *O*, in A–B–C–D quaternary system is taken for an example to deduce the expression of the Spatial Lever’s Rule under the condition of multi-phase equilibrium. First, connects

DO and extends it, crosses the plane A–B–C at point M. Second, connects AO, BO, CO, AM, BM, and CM, respectively. So DP and ON are perpendicular to plane A–B–C.

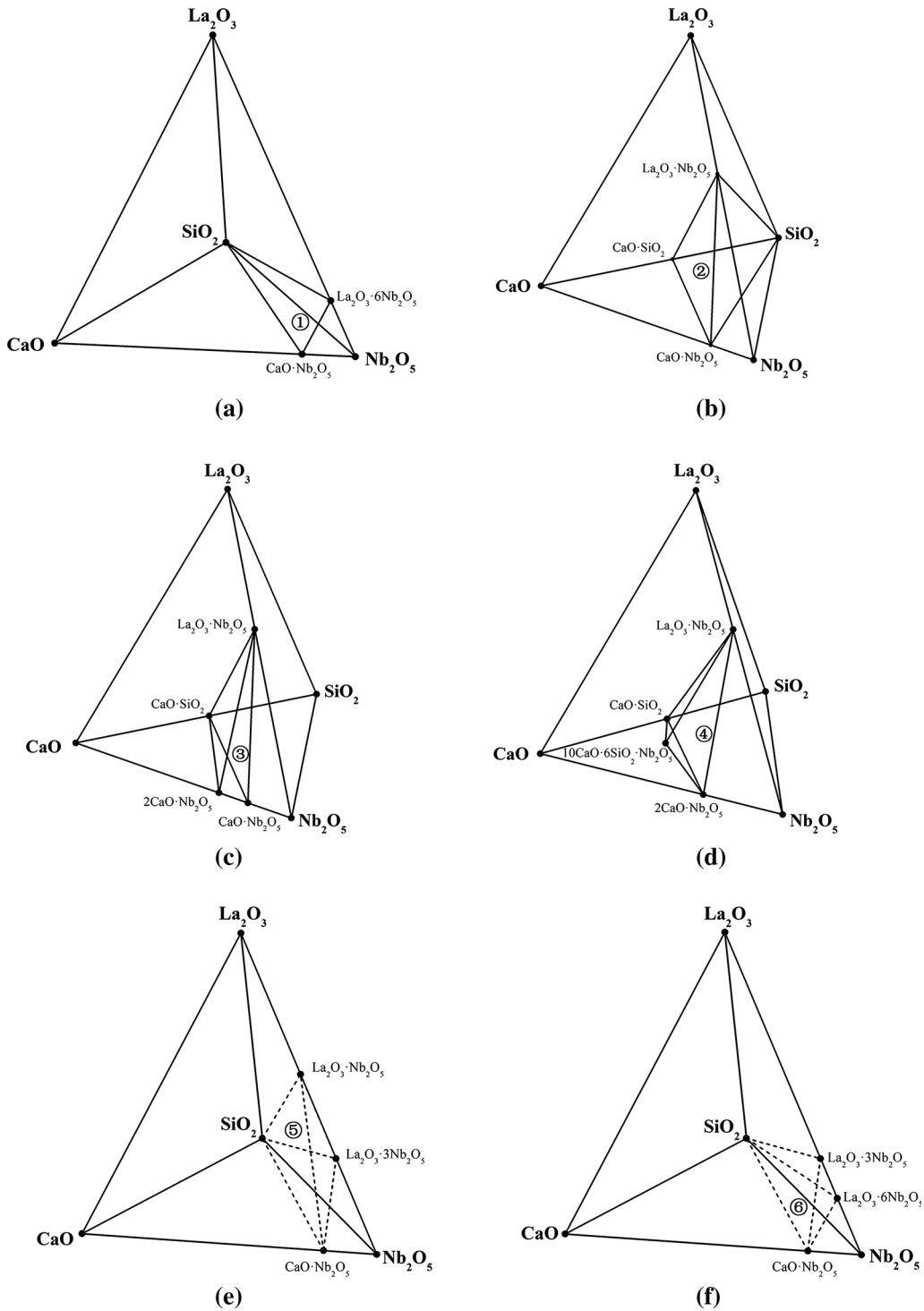


Fig. 6—Positions of the independent tetrahedrons field in the spatial quaternary phase diagram.

According to the application of the Lever's Rule when two phase equilibrium appears, the composition of point O can be expressed as Formula (4):

$$O = \frac{DO}{DM} * 100 \text{ pct} * M + \frac{OM}{DM} * 100 \text{ pct} * D. \quad [4]$$

For component point O , it can be found that the mass fraction of component M is $\frac{DO}{DM} * 100 \text{ pct}$ and the mass

fraction of phase D is $\frac{OM}{DM} * 100 \text{ pct}$. Due to the line segment ON and DP are perpendicular to plane $A-B-C$ at same time, Formulae (5) and (6) can be deduce as follow:

$$\frac{OM}{DM} = \frac{ON}{DP} = \frac{h_{\text{tetrahedron } A-B-C-O}}{h_{\text{tetrahedron } A-B-C-D}}, \quad [5]$$

$$\frac{MO}{DM} = \frac{S_{\Delta ABC} * h_{\text{tetrahedron A-B-C-O}}}{S_{\Delta ABC} * h_{\text{tetrahedron A-B-C-D}}} = \frac{V_{\text{tetrahedron A-B-C-O}}}{V_{\text{tetrahedron A-B-C-D}}} \quad [6]$$

From the Formula (3), it can be found that the mass fraction of phase D can be represented by $\frac{V_{\text{tetrahedron A-B-C-O}}}{V_{\text{tetrahedron A-B-C-D}}} * 100 \text{ pct}$, the mass fraction of other equilibrium phase can be deduced similarly.

In addition to the solid phase, the equilibrium liquid phase could also participate in the calculation process to form the apex of related tetrahedron field. In other words, it is the numerical expression of the Spatial Lever Rule. This method has been used with four-phase equilibrium, but also been used with three-phase (or less than three) equilibrium. The numbers of component in relevant formula need to be reduced and related volume ratio need to be changed to area ratio (or length ratio, corresponding to the traditional Lever's Rule) in space. In multi-component system (more than four) phase diagram, the physical meaning of the mass fraction of equilibrium phase cannot be intuitively expressed by geometric relation, but the determinant calculation method can still be used.

The results of the equilibrium experiment at 1273 K (1000 °C) of #1 slag in the CaO-SiO₂-La₂O₃-Nb₂O₅ system were taken as examples, the proportion relations of the equilibrium phases in the sample were calculated by the related determinant. The composition of La₂O₃·6Nb₂O₅, Nb₂O₅, SiO₂, and CaO·Nb₂O₅ and the initial composition of #1 slag are shown in Table VI.

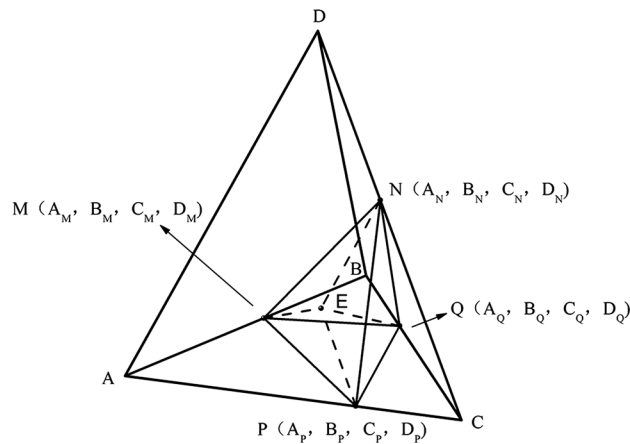


Fig. 7—A spatial illustration of the relationship in the A-B-C-D quaternary system phase diagram.

Substituting the data into Formula (1) to get Formulae (7) through (9) can be obtained simultaneously. And then, the equilibrium mass fraction of La₂O₃·6Nb₂O₅ can be calculated, the calculation of other equilibrium phases can be carried out in the same way, the results are given in Table VII.

$$V = \begin{vmatrix} 1 & 1 & 1 & 1 & 1 \\ 1.48 \text{ pct} & 0 & 0 & 10.90 \text{ pct} & 4.23 \text{ pct} \\ 0 & 0 & 100.00 \text{ pct} & 0 & 3.42 \text{ pct} \\ 14.49 \text{ pct} & 0 & 0 & 6.33 \text{ pct} & 11.29 \text{ pct} \\ 84.03 \text{ pct} & 100.00 \text{ pct} & 0 & 82.77 \text{ pct} & 81.06 \text{ pct} \end{vmatrix}, \quad [7]$$

$$\begin{aligned} V_{\text{La}_2\text{O}_3 \cdot 6\text{Nb}_2\text{O}_5} &= |A_{11}| \\ &= \begin{vmatrix} 0 & 0 & 10.90 \text{ pct} & 4.23 \text{ pct} \\ 0 & 100.00 \text{ pct} & 0 & 3.42 \text{ pct} \\ 0 & 0 & 6.33 \text{ pct} & 11.29 \text{ pct} \\ 100.00 \text{ pct} & 0 & 82.77 \text{ pct} & 81.06 \text{ pct} \end{vmatrix} \\ &= 0.00962851, \end{aligned} \quad [8]$$

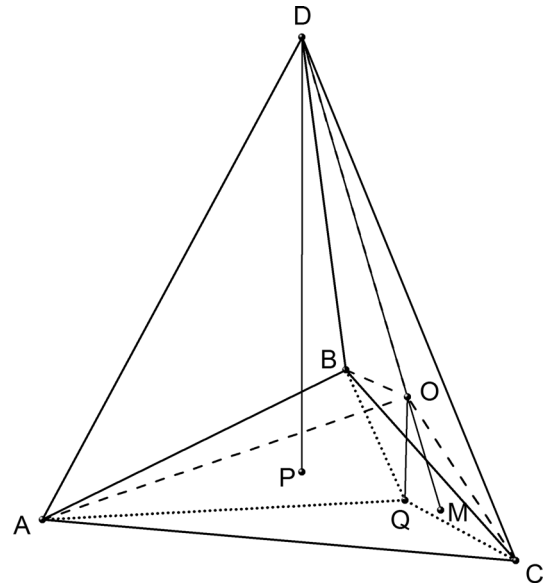


Fig. 8—Schematic diagram for deduction of Spatial Lever Rule in quaternary system.

Table V. The Theoretical Composition of Phases M, N, P, and Q

	Phase M	Phase N	Phase P	Phase Q
Mass Fraction of A	A_M	A_N	A_P	A_Q
Mass Fraction of B	B_M	B_N	B_P	B_Q
Mass Fraction of C	C_M	C_N	C_P	C_Q
Mass Fraction of D	D_M	D_N	D_P	D_Q

Table VI. The Theoretical Composition of La₂O₃·6Nb₂O₅, Nb₂O₅, SiO₂, and CaO·Nb₂O₅ and Initial Composition of slag #1

	La ₂ O ₃ ·6Nb ₂ O ₅ (Pct)	Nb ₂ O ₅ (Pct)	SiO ₂ (Pct)	CaO·Nb ₂ O ₅ (Pct)	#1 (Pct)
Mass Fraction of CaO	0	0	0	17.39	4.23
Mass Fraction of SiO ₂	0	0	100.00	0	3.42
Mass Fraction of La ₂ O ₃	16.96	0	0	0	11.29
Mass Fraction of Nb ₂ O ₅	83.04	100.00	0	82.61	81.06

Table VII. Mass Fraction of Each Equilibrium Phase of Slag #1 at 1273 K (1000 °C)

Phases	La ₂ O ₃ ·6Nb ₂ O ₅	Nb ₂ O ₅	SiO ₂	CaO·Nb ₂ O ₅
Calculation Formula	$\frac{V_{La_2O_3 \cdot 6Nb_2O_5}}{V_{\#1}} \times 100$ pct	$\frac{V_{Nb_2O_5}}{V_{\#1}} \times 100$ pct	$\frac{V_{SiO_2}}{V_{\#1}} \times 100$ pct	$\frac{V_{CaO \cdot Nb_2O_5}}{V_{\#1}} \times 100$ pct
Mass Fraction (Pct)	64.81	1.77	3.42	30.01

Table VIII. Mass Fraction of Each Equilibrium Phase of Slags #2 Through #4 at 1273 K (1000 °C)

Slag Nos.	Equilibrium Phases	Mass Fractions (Pct)
#2	CaO·Nb ₂ O ₅	14.63
	CaO·SiO ₂	56.45
	SiO ₂	5.67
#3	La ₂ O ₃ ·Nb ₂ O ₅	23.25
	CaO·SiO ₂	25.15
	CaO·Nb ₂ O ₅	55.42
#4	2CaO·Nb ₂ O ₅	7.33
	La ₂ O ₃ ·Nb ₂ O ₅	12.10
	2CaO·Nb ₂ O ₅	32.49
	CaO·SiO ₂	18.05
	10CaO·6SiO ₂ ·Nb ₂ O ₅	37.17

The mass fraction of La₂O₃·6Nb₂O₅ can be obtained by $V_{La_2O_3 \cdot 6Nb_2O_5}/V_{\#1}$. Similarly, we can get $V_{Nb_2O_5} = |A_{12}| = 0.00026228$, $V_{SiO_2} = |A_{13}| = 0.000508118$, $V_{CaO \cdot Nb_2O_5} = |A_{14}| = 0.00445835$. The value of the determinants is numerically satisfied with $V_{La_2O_3 \cdot 6Nb_2O_5} + V_{Nb_2O_5} + V_{SiO_2} + V_{CaO \cdot Nb_2O_5} = V_{\#1}$. Further calculation results are given in Table VII. The mass fraction of equilibrium phases of sample #1 at 1273 K were calculated by this method.

The mass fraction of equilibrium phases of samples #2, #3, and #4 at 1273 K were calculated respectively at same time, the results were given in Table VIII. All equilibrium phases were converted to initial composition according to their mass fraction and composition, the comparison between initial composition measured by EDS and calculated by conversion were given in Table IX. It was found that the results showed good consistency.

$$V_{\#1} = |V_{15}|$$

$$= \begin{vmatrix} 1.48 \text{ pct} & 0 & 0 & 10.90 \text{ pct} \\ 0 & 0 & 100 \text{ pct} & 0 \\ 14.49 \text{ pct} & 0 & 0 & 6.33 \text{ pct} \\ 84.03 \text{ pct} & 100 \text{ pct} & 0 & 82.77 \text{ pct} \end{vmatrix} \quad [9]$$

$$= 0.01485726.$$

IV. CONCLUSION

High-temperature equilibrium experiment has been applied to investigate the equilibrium phase relations and the corresponding proportion relations in the CaO-SiO₂-Nb₂O₅-La₂O₃ system at 1273 K (1000 °C). According to the Gibbs Phase Rule, six independent tetrahedron fields in the CaO-SiO₂-Nb₂O₅-La₂O₃ system were determined. A numerical method for quantitatively

Table IX. The Comparison Between Composition of Slags #1 Through #4 by Measured and by Calculated (Mass Percent)

Slag Nos.	CaO (Pct)	SiO ₂ (Pct)	Nb ₂ O ₅ (Pct)	La ₂ O ₃ (Pct)
#1	calculated	4.23	3.42	11.29
	measured	4.23	3.42	11.29
#2	calculated	26.89	38.53	12.16
	measured	26.89	38.53	12.16
#3	calculated	20.08	12.87	10.08
	measured	20.08	12.87	10.08
#4	calculated	30.74	20.94	9.77
	measured	30.74	20.94	9.77

analyzing the proportion relation of equilibrium phases in multi-component system was deduced. The mass fraction of each equilibrium phase in each experimental slag in the CaO-SiO₂-Nb₂O₅-La₂O₃ system at 1273 K was calculated, respectively.

ACKNOWLEDGMENTS

This work was financially supported by the National Key R&D Program of China (No. 2017YFC0805105), National Natural Science Foundation of China (No. 51774087), the Fundamental Research Funds for the Central Universities China (No. N162506002).

REFERENCES

1. J. Ren, G. Xu, and W. Wang: *Technology and Application of Niobium Mining and Metallurgy*, 1st ed., Nanjing University Press, Nanjing, 2001, pp. 1–277.
2. S. Li, Y. Zhou, H. Du, and G. Qian: *Development and Application Technology of Niobium Resources*, 1st ed., Metallurgical Industry Press, Beijing, 1992, pp. 3–226.
3. A. Jongejan and A.L. Wilkins: *J. Less-Common Met.*, 1969, vol. 19, pp. 203–08.
4. J. Shi, L. Sun, B. Zhang, X. Liu, J. Qiu, Z. Wang, and M. Jiang: *Metall. Mater. Trans. B*, 2016, vol. 47B, pp. 425–33.
5. J. Shi, L. Sun, J. Qiu, Z. Wang, B. Zhang, and M. Jiang: *ISIJ Int.*, 2016, vol. 56, pp. 1124–31.
6. J. Shi, L. Sun, J. Qiu, B. Zhang, and M. Jiang: *J. Alloys Compd.*, 2017, vol. 699, pp. 193–99.
7. L. Sun, J. Shi, B. Zhang, J. Qiu, Z. Wang, and M. Jiang: *J. Cent. South Univ. (Engl. Ed.)*, 2017, vol. 24, pp. 48–55.
8. Z. Guo, D. Yan, and Z. Lin: *High Temperature Phase Equilibrium and Phase Diagram*, 1st ed., Shanghai Scientific Technical Publishers, Shanghai, 1987, pp. 107–18.
9. H.M. Henao and F. Kongoli: *Mater. Trans.*, 2005, vol. 46, pp. 812–19.
10. H.M. Henao, C. Pizarro, J. Font, A. Moyano, P.C. Hayes, and E. Jak: *Metall. Mater. Trans. B*, 2010, vol. 41B, pp. 1186–93.
11. S.S. Pandit and K.T. Jacob: *Metall. Mater. Trans. B*, 1995, vol. 26B, pp. 397–99.
12. R. Zhang and P. Taskinen: *J. Alloys Compd.*, 2016, vol. 657, pp. 770–76.
13. A.M. Frolov and A.A. Evdokimov: *Russ. J. Inorg. Chem.*, 1987, vol. 32, pp. 1771–73.
14. E.H. Nickel: *Am. Mineral.*, 1956, vol. 41, pp. 785–86.
15. C. Liu: *Phase Rule and Phase Diagram Thermodynamics*, 1st ed., Higher Education Press, Beijing, 1995, pp. 27–33.
16. M. Ibrahim, N.F.H. Bright, and J.F. Rowland: *J. Am. Ceram. Soc.*, 1962, vol. 45, pp. 329–34.
17. M. Ibrahim and N.F.H. Bright: *J. Am. Ceram. Soc.*, 1962, vol. 45, pp. 221–22.